Solvation Effects on Reaction Profiles by the Polarizable Continuum Model Coupled with the Gaussian Density Functional Method

TZONKA MINEVA, NINO RUSSO, EMILIA SICILIA

Dipartimento di Chimica, Università della Calabria, I-87030 Arcavacata di Rende (CS), Italy

Received 22 February 1997; accepted 23 August 1997

ABSTRACT: An efficient version of the polarizable continuum model for solvation has been implemented in the Gaussian density-functional-based code called deMon. Solvation free energies of representative compounds have been calculated as a preliminary test. The hydration effects on the reaction profile of the $Cl^- + CH_3Cl \rightarrow ClCH_3 + Cl^-$ reaction and the thermodynamics of the Menschutkin reaction have also been investigated. Finally, the conformational behavior of the 1,2-diazene cis–trans isomerization process in water was examined. Comparisons between the results obtained and the available experimental data and previous theoretical computations have been made.
 J Comput Chem 19: 290–299, 1998

Keywords: solvation; density functional; polarizable continuum model (PCM); reaction profiles; hydration energy

Introduction

The possibility of theoretical estimation of solvent effects on the properties of molecules remains a challenge in computational chemistry because the majority of chemically and biologically important reactions occur in solution. Starting from Laplace's (or Poisson's) equation, under given boundary conditions, different self-consistent reaction field (SCRF) continuum models have been proposed.[1–4] In this approach the solute, treated quantum-mechanically, is placed in a cavity surrounded by the solvent, considered as a continuum characterized by one or more of its bulk properties. The idea of modeling the electrostatic portion of solvation by placing the solute in a cavity of the solvent dates back to the works of Onsager[5] and Kirkwood[6] on solvation effects in polar molecules. The subsequent history of continuum models has been recently exhaustively reviewed.[1–3]

Correspondence to: T. Mineva
Contract/grant sponsors: MURST; CNR; CINECA

CCC 0192-8651 / 98 / 030290-10

The polarizable continuum model (PCM), developed by Tomasi and coworkers,[7,8] allows one to work with cavities of realistic molecular shape, with the surface of the cavity being tassellated into spherical polygons. The solute–solvent electrostatic interaction is described by a set of polarization point charges, placed in the center of each tessera. It should therefore be more versatile in terms of a realistic description of the cavity and an accurate evaluation of the solute–solvent interaction energy.

The PCM was originally implemented[7] in the framework of the Hartree–Fock (HF) theory and successively modified to take into account correlation effects.[8–10]

On the other hand, the Kohn–Sham formalism of the density functional theory (DFT), including gradient corrections, has been shown to be a useful alternative to post-HF methods for the reliable prediction of molecular properties with relatively low computational cost.[11–13] It is, therefore, of theoretical and practical interest to implement continuum models in the framework of DFT.

The use of DFT coupled with PCM has already been considered,[14–18] but the majority of the applications concerns benchmarks on the solvation energies of representative molecules. To our knowledge, studies carried out using the PCM tool in the framework of DFT, of other significant chemical properties (e.g. relative stability and reaction paths), are very scarce.[14]

In this context we have considered it of interest to implement the most recent PCM procedure in the Gaussian density functional code, deMon,[19] and to extend its range of applications.

We first tested the reliability of the coupling between DFT and PCM carrying out the computation of the solvation free energies of a series of organic molecules and ions. This step was necessary because the reliability, in solvent, of the local and gradient-corrected exchange-correlation functionals used by us was never verified. Solvation free energies were then calculated along the pathway of model S_N2 type I and type II reactions and for the trans–cis isomerization process of diazene.

Method

Within the density functional theory, an N-electron system is represented by a Hamiltonian:

$$H^0 = T + V + U$$

where T is the operator corresponding to the kinetic energy, V is the external potential operator, and U that for the electron–electron repulsion. The conventional approach is to insert this Hamiltonian into the Schrodinger equation to obtain:

$$E = T[\,\rho] + \int V(\mathbf{r})\rho(\mathbf{r})\,dr + \frac{1}{2}\int \rho(\mathbf{r})\rho(\mathbf{r}')\,d\mathbf{r}\,d\mathbf{r}' + E_{XC}[\,\rho] \quad (1)$$

where $E_{XC}[\,\rho]$ represents the exchange-correlation energy for the electron density, ρ, and the third term is the Coulomb interaction energy.

Applying the variational principle $\delta E/\delta\rho = 0$ to eq. (1) yields the Kohn–Sham equations[20] for the one-electron orbital, ψ_i:

$$\left[-\frac{1}{2}\nabla^2 + V(\mathbf{r}) + \int \frac{\rho(\mathbf{r}')}{|\mathbf{r}-\mathbf{r}'|}\,d\mathbf{r}' + \frac{\delta E_{XC}}{\delta\rho}\right]\psi_i = \varepsilon_i\psi_i \quad (2)$$

the density being given simply by:

$$\rho(\mathbf{r}) = \sum_i n_i\psi_i^*(\mathbf{r})\psi_i(\mathbf{r}) \quad (3)$$

where n_i is the occupation number.

In the PCM, the solute is represented by a charge distribution in a cavity embedded in an infinite polarizable dielectric medium with permittivity ε. This molecular charge induces a reaction potential in the medium, which acts back on the charge distribution itself, producing in turn changes in the initial gas phase distribution. The Hamiltonian of the solute is expressed as:

$$H = H^0 + V\sigma \quad (4)$$

where H^0 is the Hamiltonian of the solute molecule *in vacuo* and $V\sigma$ is the perturbation term representing the effect of the reaction field. The solution of the Schrodinger equation:

$$(H^0 + V_\sigma)|\Psi'\rangle = E|\Psi'\rangle \quad (5)$$

gives, as output, the total (electronic and nuclei) charge distribution on which $V\sigma$ depends.

To solve this implicit problem, the original formulation[7] adopted an iterative procedure based on a discretization of the problem. In fact, the presence of a cavity of irregular shape imposes boundary conditions that make it difficult to obtain directly the solution of the integral-differential equation [eq. (5)].

A finite set of surface charges is introduced, q_i, each associated with a small portion (tessera), with

area ΔS_i, of the cavity surface:

$$q_i = \sigma(\mathbf{s}_i)\,\Delta S_i \tag{6}$$

where $\sigma(\mathbf{s}_i)$, which is the apparent charge distribution at the representative point, $\mathbf{s}_i$, within the tessera, i, has the implicit definition:

$$\sigma(\mathbf{s}) = -\frac{\varepsilon - 1}{4\pi\varepsilon}\mathbf{E} \tag{7}$$

In this equation, **E** represents the normal component of the total electric field, on the inner side of the cavity surface, which has two sources in the solute and the apparent surface charge distribution.

The reaction potential of the solvent, $V\sigma$, also assumes a discrete form:

$$V_\sigma = \sum_i \frac{q_i}{|\mathbf{r} - \mathbf{s}_i|} \tag{8}$$

Once this discretization is done, a first guess of the q_i values is obtained by using the potential due to solute charge distribution *in vacuo* as the provisional value and then performing an iterative calculation.

An alternative approach to the iterative one is offered by a matrix formulation (BEM)[21,22] of the electrostatic problem. Eq. (6) can be put in the following matrix form:

$$\mathbf{Dq} = -\Sigma\mathbf{E_n} \tag{9}$$

where **D** is a square matrix with dimension equal to the number of tesserae; Σ is a square diagonal matrix, with the same dimension of **D**, with elements equal to the area of the tesserae, $\Delta\Sigma_i$; and $\mathbf{E_n}$ is the column matrix of the normal components of the electric field. In the BEM version we used here, the **D** matrix is inverted and kept in memory to be used for all the quantum cycles and the **q** charges obtained directly by matrix multiplication:

$$\mathbf{q} = -\mathbf{D}^{-1}\Sigma\mathbf{E_n} \tag{10}$$

The solute cavity surface is modeled by the union of spheres centered on the solute atoms and tassellated following the GEPOL[23] procedure and adding the possibility of analytically calculating the surface of the tesserae lying at the intersection of two or more spheres with the Gauss–Bonnet theorem.[24]

Up to now we have only considered the electrostatic component of the total solvation free energy, ΔG_{solv}, which can be evaluated from the sum of the following contributions[3]:

$$\Delta G_{solv} = \Delta G_{el} + \Delta G_{cav} + \Delta G_{disp} + \Delta G_{rep} \tag{11}$$

where ΔG_{el} is the electrostatic contribution, ΔG_{cav} is a positive term corresponding to the work spent in forming a suitable cavity in the medium, ΔG_{disp} is the dispersion contribution due to the coupling work, and ΔG_{rep} is a repulsion term due to the noncovalent interactions.

The cavitation contribution is calculated applying Pierotti's[25] formulation adapted to take into account the description of molecules in terms of overlapping spheres:

$$\Delta G_{cav} = \sum_i^{\text{spheres}} \frac{A_i}{4\pi\bar{R}_i^2}\Delta G_{cav}(R_i) \tag{12}$$

where each sphere, with radius R_i and cavitation energy $\Delta G_{cav}(R_i)$, contributes with a weight depending on the portion of its surface exposed to the solvent (A_i).

The dispersion–repulsion terms are calculated adopting the atom–atom potential parameters proposed by Caillet and Claverie[26] in the procedure reported in ref. 27.

The computations were carried out employing both the local Vosko, Wilk, and Nusair (VWN)[28] and the gradient-corrected exchange and correlation potentials of Perdew and Wang[29] and Perdew[30] (PP), respectively. The triple-zeta plus polarization orbital basis set, with corresponding auxiliary basis functions, was employed.[31] The geometries of all compounds considered were fully optimized in the gas phase and without symmetry constraints by using the Broyden–Fletcher–Goldfarb–Shanno algorithm.[32]

The same gas phase geometries were used to calculate the energies in solvent.

Results and Discussion

HYDRATION (ΔG_{hyd}) FREE ENERGY

As a first step to test the performance of our approach we carried out computation of the hydration (ΔG_{hyd}) free energy for a series of representative neutral and charged molecules for which experimental[33–35] data are available. Results are shown in Table I.

As is well known, a critical factor of the method is the choice of shape and the size of the cavity, which should reproduce the shape of the solute

with the inclusion of the whole charge distribution and with the exclusion of empty spaces.

In the original version[7] of PCM the cavity was defined in terms of spheres with radii R, proportional to the van der Waals radii, $R = fR^{vdW}$. The initially proposed proportionality factor, for the evaluation of the electrostatic term with neutral solutes, was $f = 1.2$. In our calculations, we adopted the same factor for both neutral and charged species. Moreover, we tested the performance of the method with the two most popular sets of reference atomic radii, namely the Bondi[36] and Pauling[37] sets. The best results (see Table I) were obtained by using the Pauling set, except for hydrogen atoms bound to eteroatoms, which have a radius value of 1 Å. Employing the Bondi set, at the nonlocal level, the electrostatic contribution was found to be underestimated by about 2 kcal/mol for most of the species examined (e.g., the ΔG_{el} values of NH_3, CH_3OH, and CH_3CONH_2 were -4.1, -4.2, and -10.5 kcal/mol, respectively). To get ΔG_{hyd} closer to experimental results, the computation of nonelectrostatic terms, which require cavities of different size with respect to electrostatic ones,[2] was performed using the same set of unscaled radii. All solvation free energies reported in this study were calculated using this set of radii.

It is worth noting that the local VWN functional is able to give enough correct hydration free energies.

Except for CH_3NH_2 and CH_3COOH molecules, the agreement with the experimental values was good and comparison with previous DFT studies[15,18] was satisfactory for both neutral and charged species.

SOLVATION EFFECTS ON MODEL S_N2 REACTIONS

The bimolecular nucleophilic substitution reaction is one of the most fundamental processes in organic chemistry and has been used extensively as a model in studies involving solvation effects.

In this article, we report our results for the prototypical type I $Cl^- + CH_3Cl \rightarrow ClCH_3 + Cl^-$ and type II Menschutkin S_N2 reactions.

The fact that gas phase and aqueous solution rates for the S_N2 $Cl^- + CH_3Cl \rightarrow ClCH_3 + Cl^-$ reaction differ by 20 orders of magnitude is one of the clearest examples of the notable influence of solvation on kinetics of reactive processes in the condensed phase.

Geometrical parameters of stationary points along the reaction path, namely the CH_3Cl molecule, $Cl^- \cdots CH_3Cl$ ion dipole complex, and

TABLE I.
Hydration Free Energies (Kilocalories per Mole) for a Set of Test Compounds from VWN and PP Computations.

System	ΔG_{el} VWN	ΔG_{el} PP	ΔG_{rep}	ΔG_{dis}	ΔG_{cav}	ΔG_{hyd} VWN	ΔG_{hyd} PP	ΔG_{hyd}[a]	ΔG_{hyd}[b]	ΔG(exp)[c]
H_2O	−8.7	−8.3	0.8	−3.9	4.5	−7.3	−6.9	−7.1	−7.4	−6.3
CH_4	−0.3	−0.2	1.0	−6.3	7.0	1.5	1.6			2.0
HCN	−5.8	−5.5	1.1	−5.6	6.0	−4.3	−4.1	−4.2		−3.2
NH_3	−6.5	−6.2	0.8	−4.4	5.1	−5.1	−4.7	−4.8	−5.2	−4.3
CH_3OH	−6.2	−5.9	1.3	−7.8	8.1	−4.6	−4.3	−4.4	−4.1	−5.1
CH_3CN	−6.5	−6.1	1.4	−8.5	9.2	−4.4	−4.0	−5.1	−4.6	−3.9
CH_3CH_3	−0.6	−0.5	1.3	−8.8	10.5	2.4	2.5	2.0		1.8
CH_3NH_2	−5.6	−5.3	1.2	−7.8	8.8	−3.4	−3.1	−3.0	−2.8	−4.6
CH_3CHO	−5.8	−5.6	1.4	−9.0	10.1	−3.3	−3.1	−3.7		−3.7
CH_3COOH	−8.8	−8.4	1.6	−10.0	11.3	−5.9	−5.5	−6.1	−5.8	−6.7
CH_3CONH_2	−12.5	−12.3	1.6	−10.3	12.1	−9.2	−9.0	−9.0		−9.7
CH_3COCH_3	−6.5	−6.3	1.6	−11.5	12.8	−3.6	−3.4	−3.0	−2.0	−3.8
NO_3^-	−67.9	−67.0	1.4	−7.3	7.9	−65.9	−65.0			−65.0
NH_4^+	−78.2	−77.8	1.0	−5.9	6.7	−76.4	−76.0			−79.0
CH_3COO^-	−74.8	−74.4	1.4	−9.8	10.7	−72.5	−72.1		−72.0	−74.1
$CH_3NH_3^+$	−76.4	−75.9	1.2	−8.1	9.4	−73.9	−73.4		−74.1	−74.5

[a] From ref. 15.
[b] From ref. 18.
[c] From refs. 33 and 34 for neutrals, ref. 35 for ions.

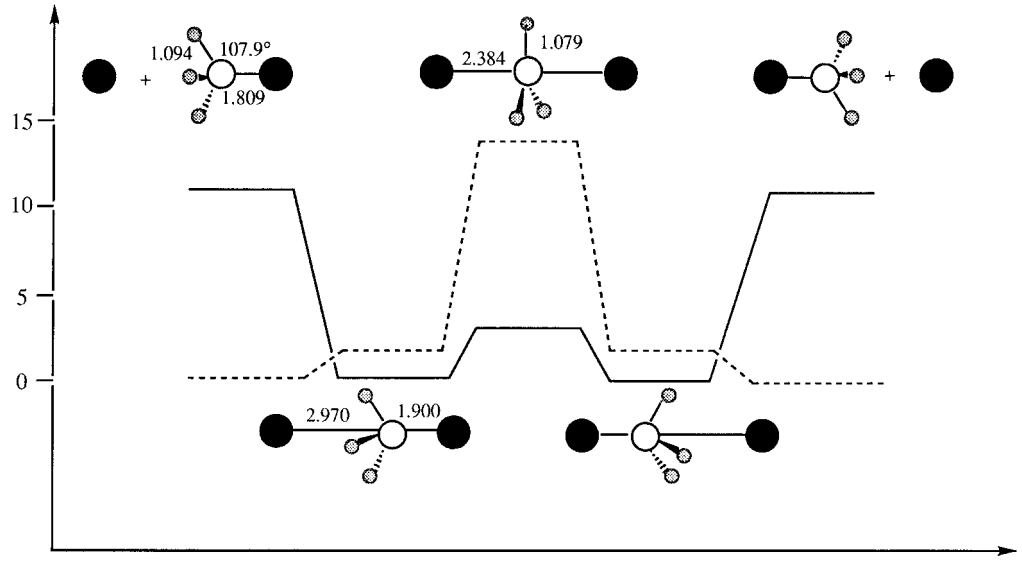

FIGURE 1. Reaction profile of the $S_N2Cl^- + CH_3Cl$ reaction in the gas phase (solid line) and in aqueous solution (dashed line). The reported geometrical parameters are expressed in angstroms for bond lengths and degrees for angles.

$[Cl \cdots CH_3 \cdots Cl]^-$ transition state, are reported in Figure 1.

Among the numerous theoretical studies[38–42] on the gas phase double-well-energy profile of this reaction, that by Deng et al.[42] provides a critical analysis on the performance of DFT in calculating transition state properties for this kind of S_N2 reaction. In fact, while a barrier of 3.1 kcal/mol is predicted by fitting a semiempirical analytical potential energy function[39] to the experimental thermal rate constant,[43] the barrier height calculated at the nonlocal level is noticeably underestimated and a negative value of −8.0 kcal/mol indicates that the transition state is below the separated reactants. The difference in energy between the separate reactants and the complex is 11.0 kcal/mol as opposed to an experimental value of 8.6 ± 0.2 kcal/mol.[44]

The calculated reaction profile (Fig. 1) for the solution case was found to have a unimodal shape consistent with experimental observations,[45,46] but, quantitatively, the calculated barrier height of 14.0 kcal/mol was too low with respect to the experimental estimate of 26 kcal/mol.[45,46] Values ranging from 16.0 to 24.3 kcal/mol were obtained from a study using a generalized conductor-like screening model within Hartree–Fock, MP2, and hybrid DFT quantum-mechanical approaches.[47] Nevertheless, this comparison is somewhat misleading because the error for the gas phase barrier is also included. In estimating the solvent contribution to the barrier height as the difference between the experimental liquid phase (26 kcal/mol) and semiempirical gas phase (3.1 kcal/mol) barriers, we found very good agreement (22.4 vs. 22.9 kcal/mol). Further analysis showed that hydration free energies of reactants (see Table II) were also well reproduced.

Another important process to quantify the influence of the solvent on the chemical reactivity is the

TABLE II.
Electrostatic and Nonelectrostatic Contributions (Kilocalories per Mole) to Calculated Free Energies of Hydration for Species Involved in the S_N2 Type I Reaction Considered.

System	ΔG_{el}	ΔG_{rep}	ΔG_{dis}	ΔG_{cav}	ΔG_{hyd}	$\Delta G(exp)^a$
Cl^-	−74.4	1.0	−4.6	4.9	−73.1	−75.0
CH_3Cl	−2.7	1.5	−8.3	9.1	−0.4	0.6
$Cl^- \cdots CH_3Cl$	−64.7	2.0	−11.0	13.4	−60.3	
$[Cl \cdots CH_3 \cdots Cl]^-$	−55.3	2.0	−10.9	13.3	−50.9	

[a] From ref. 46

so-called Menschutkin reaction $NH_3 + CH_3Cl \rightarrow CH_3NH_3^+ + Cl^-$.

Because of the large expected structural changes for transition state we considered only minima along the reaction path.

In the gas phase we found an endothermicity of 118.0 and 120.0 kcal/mol at local (VWN) and nonlocal (PP) levels, respectively. The corresponding MP4/6-31G* value and the experimental one, computed from standard free energies of formation, were 119.0 and 110.0 kcal/mol, respectively.[48,49]

The presence of solvent had a dramatic effect. In water the reaction was exothermic by 22.5 (local) and 17.9 (nonlocal) kcal/mol, which represents a solvent stabilization of about 136 and 138 kcal/mol

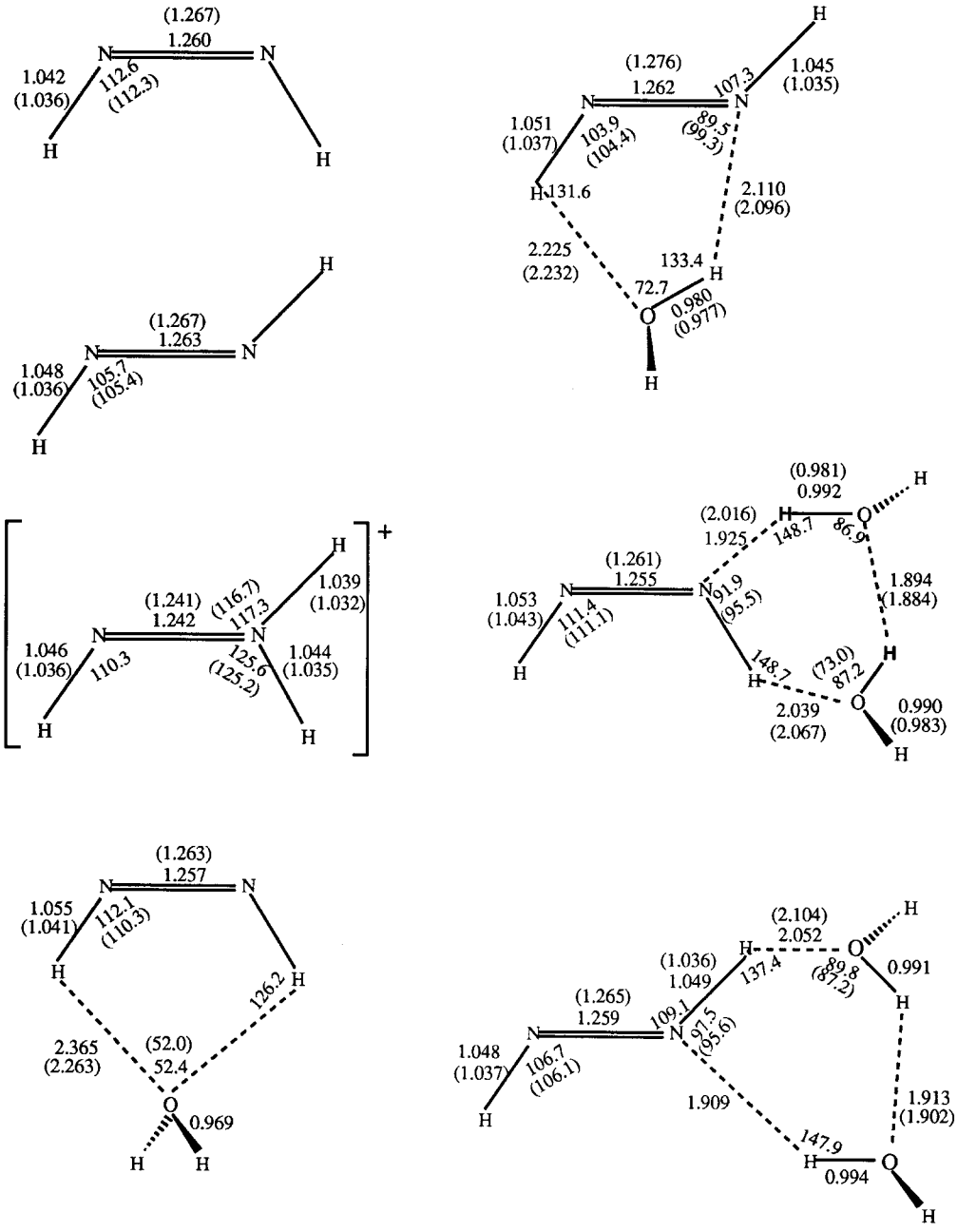

FIGURE 2. PP-optimized molecular structures of species involved in the isomerization process of 1,2-diazene. Bond distances are in angstroms and angles in degrees. In parentheses are reported some of the MP2 geometrical parameters for comparison with ref. 55.

relative to the gaseous process. *Ab initio*–correlated computations[50] yielded values ranging from −27 to −44 kcal/mol, depending on the basis set employed, whereas a combined quantum-mechanical and molecular-mechanical model gave[51] −18 kcal/mol and a corrected value of −36 kcal/mol, taking into account overestimation of heat of formation of Cl^-. The experimental estimation of the free energy of reaction in water, from a thermodynamic cycle using free energies of hydration and standard free energies of formation, was -34 ± 10 kcal/mol.[48] The range of theoretical and experimentally estimated values was too large to make a comparison, although our results suggested that the reaction, extremely unfavorable and never observed in the gas phase,[52] became exothermic in aqueous solution.

CIS–TRANS ISOMERIZATION OF 1,2-DIAZENE

Because 1,2-diazene is believed to be an intermediate in some oxidations of hydrazine and to be able to stereospecifically reduce the olefinic bond via an allowed pericyclic reaction, it was indisputably characterized in the gas phase and its chemistry in water and other solvents has been reviewed extensively.[53] Direct detection of aqueous 1,2-diazene comes from UV spectra in the acid-assisted hydrolysis of azodiformate.[54] Because of the difficulty in observing this species in aqueous media (due to its rapid decomposition in N_2 and N_2H_4), theoretical studies are useful for better characterization as well as for a contribution to the interpretation of the experimental data. In particular, it is necessary to pay attention to solvent effects to explain why *trans*-N_2H_2 decomposes rapidly in the gas phase, whereas it undergoes isomerization in solution.

Previous in-solution studies have been performed on the cis–trans isomerization process of N_2H_2 in aqueous solution using the AM1–SM2 method combined with *ab initio* results.[55] Thus, a full *ab initio*–correlated study of solvent effects on the thermodynamics of this reaction does not exist in the literature.

We have considered the cis–trans isomerization process both in the gas phase and in an aqueous environment. Because it is believed that water plays an active role in this reaction we have also explicitly considered H_2O–N_2H_2 supermolecules. Thus, the studied reactions for the cis–trans isomerization process of 1,2-diazene are:

(a) *trans*-$N_2H_2 \rightarrow$ *cis*-N_2H_2

(b) *trans*-$N_2H_2 + H_2O \rightarrow$ *cis*-$N_2H_2 + H_2O$

(c) *trans*-$N_2H_2 + H_2O \rightarrow N_2H_3^+ + OH^- \rightarrow$ *cis*-$N_2H_2 + H_2O$

(d) *trans*-$N_2H_2 + H_3O^+ \rightarrow N_2H_3^+ + H_2O \rightarrow$ *cis*-$N_2H_2 + H_3O^+$

The gas phase geometries are reported in Figure 2. Comparisons for diazene–water complexes, possible only with previous theoretical data, show that our PP structures were very close to those obtained at the MP2 level of theory.[55] Relative energies in the gas phase and in water solvent of the various species involved in reactions (a)–(d) are shown in Table III, whereas the corresponding

TABLE III.
Relative Energies of Various Species Involved in cis – trans Isomerization of 1,2-Diazene (Kilocalories per Mole). MP4, QCISD(T), and AM1-SM2 Data Are Taken from Ref. 55.

System	PP[a]	MP4[a]	QCISD(T)[a]	PP[b]	AM1-SM2[b]
trans-N_2H_2	0.0	0.0	0.0	0.0	0.0
cis-N_2H_2	4.7	6.0	5.8	7.3	7.0
trans-$N_2H_2 + H_2O$	0.0	0.0	0.0	0.0	0.0
trans-$N_2H_2 \cdot H_2O$	−7.6	−7.7	−7.5	7.1	3.6
cis-$N_2H_2 \cdot H_2O$	−1.3	−1.3	−1.4	13.8	6.4
$N_2H_3^+ + OH^-$	211.4	240.2	239.6	43.5	18.5
trans-$N_2H_2 + 2H_2O$	0.0	0.0	0.0	0.0	0.0
trans-$N_2H_2 \cdot 2H_2O$	−18.8	−18.8	−14.4	13.3	7.2
cis-$N_2H_2 \cdot 2H_2O$	−15.5	−13.2	−13.1	14.3	11.3

[a]Gas phase.
[b]Aqueous solution.

solvation free energies are give in Table IV. In the gas phase, the isolated N_2H_2 preferred the trans conformation over the cis one by 4.7 kcal/mol. The corresponding values obtained at MP4 and QCISD(T) levels of theory[55] were 6.0 and 5.8 kcal/mol respectively. The cis–trans energy gap increased to 6.2 kcal/mol by the coordination of one water molecule, whereas it was reduced to 3.3 kcal/mol by the presence of two water molecules, probably because of the strong interaction with the permanent dipole of *cis*-N_2H_2 isomer.

Due simply to the significant dipole moment of *cis*-N_2H_2 it might be expected that solvation would reduce the energy difference. However, solvation free energies also favored the trans isomer in all cases, in agreement with the experimental measurements that indicate the trans form to be more stable over the cis in both the gas phase[56] and in aqueous solution.[54] In fact, the ΔG_{hyd} was -13.4 and -11.3 kcal/mol for the trans and cis conformers, respectively, thus the energy difference became 7.3 kcal/mol. This effect can be tied to the contribution of quadrupolar moment that is sensibly greater for the trans form, as confirmed by a test performed by us using an extended Onsager approach.[57]

Considering reaction (c), we found that the formation of the $N_2H_3^+ + OH^-$ was substantially stabilized in solution because of the formation of two ionic species but, notwithstanding a solvation energy of -191.3 kcal/mol, the process was endothermic by 43.5 kcal/mol. This value, sensibly higher than the corresponding AM1–SM2 value,[55] could exclude the possibility that isomerization takes place via this mechanism.

Figure 3 shows the energetic behavior of reaction (d) in gas phase and in solution. In the gas phase, the formation of $N_2H_3^+$ cation, via proton transfer from H_3O^+ to *trans*-N_2H_2, was exothermic of -19.2 kcal/mol, but deprotonation to obtain the cis isomer was endothermic by 23.9 kcal/mol. In aqueous medium, the proton transfer from $N_2H_3^+$ to give *trans*-N_2H_2 became endothermic (7.1 kcal/mol), whereas the products of deprotonation to yield *cis*-N_2H_2 had about the same energy value ($\Delta E = 0.2$ kcal/mol). This result supports the hypothesis that proton exchange can be responsible for isomerization of diazene.

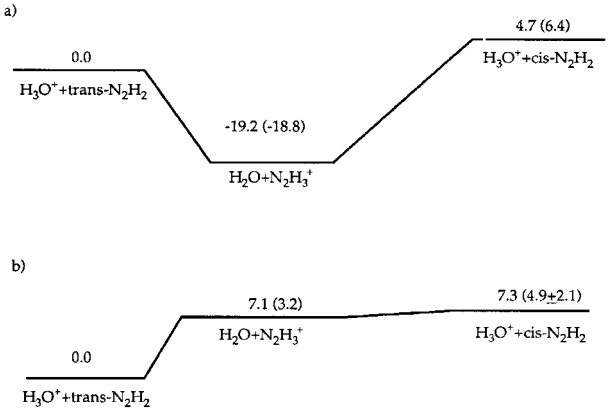

FIGURE 3. Relative energies (kilocalories per mole) of protonated / neutral pairs, H_3O^+/ N_2H_2 and $N_2H_3^+$ / H_2O, in the gas phase (a) and in aqueous solution (b). The values in parentheses are taken from ref. 55.

TABLE IV.
Solvation Free Energies (Kilocalories per Mole) of Various Species Involved in Cis – Trans Isomerization of 1,2-Diazene (Kilocalories per Mole) Calculated at PP Level.

System	ΔG_{el}	ΔG_{rep}	ΔG_{dis}	ΔG_{cav}	ΔG_{hyd}	$\Delta G_{AM1-SM2}$[a]
trans-N_2H_2	−15.7	1.0	−3.7	4.5	−13.9	−9.6
cis-N_2H_2	−13.2	1.1	−3.5	4.3	−11.3	−9.0
trans-$N_2H_2 \cdot H_2O$	−9.7	1.4	−7.7	10.0	−6.0	−12.6
cis-$N_2H_2 \cdot H_2O$	−9.5	1.4	−7.9	10.5	−5.5	−11.8
trans-$N_2H_2 \cdot 2H_2O$	−11.5	1.9	−11.0	14.5	−6.1	−14.9
cis-$N_2H_2 \cdot 2H_2O$	−10.7	1.9	−10.7	13.8	−5.7	−14.1
$N_2H_3^+$	−85.2	1.1	−5.9	6.7	−83.3	−89.5
OH^-	−109.4	1.2	−4.0	4.2	−108.0	−105.5
H_3O^+	−105.0	1.2	−4.5	4.8	−103.5	−104.2

[a]AM1–SM2 data are taken from ref. 55.

Conclusions

The polarizable continuum model for taking into account solvent effects has been implemented in the Gaussian density-functional-based code deMon. Results for hydration effects on reaction profiles are very encouraging and suggest that the computational method employed can be considered reliable and computationally economical for reaction modeling in solution.

To fully investigate reactions in solution requires the introduction of analytic calculations of energy gradients to locate critical points. Work in this area is currently in progress.

Acknowledgments

We thank Dr. Maurizio Cossi and Prof. J. Tomasi for providing us with the most recent version of the PCM codes developed by the Pisa group.

References

1. C. J. Cramer and D. Truhular, In *Quantitative Treatments of Solute/Solvent Interactions, Vol. 1,* P. Politzer and J. S. Murray, Eds., Elsevier, New York, 1994, p. 9.
2. J. Tomasi and M. Persico, *Chem. Rev.*, **94,** 2027 (1994).
3. H. Agren and K. V. Mikkelsen, *J. Mol. Struct.* (*Theochem*), **234,** 425 (1991).
4. G. De Luca, T. Mineva, N. Russo, E. Sicilia, and M. Toscano, In *Recent Advances in Density Functional Methods, Vol. 2*, D. P. Chong, Ed., World Scientific, Singapore, 1997, pp. 41–59.
5. L. Onsager, *J. Am. Chem. Soc.*, **58,** 1486 (1936).
6. J. G. Kirkwood, *J. Chem. Phys.*, **7,** 911 (1939).
7. S. Miertus, E. Scrocco, and J. Tomasi, *Chem. Phys.*, **55,** 117 (1981).
8. M. A. Aguilar, F. J. Olivares del Valle, and J. Tomasi, *Chem. Phys.*, **98,** 7375 (1993).
9. (a) M. Persico and J. Tomasi, *Croat. Chim. Acta*, **57,** 1395 (1984); (b) E. L. Coitino, J. Tomasi, and O. Ventura, *J. Chem. Soc. Faraday Trans.*, **90,** 1745 (1994).
10. F. J. Olivares del Valle and J. Tomasi, *Chem. Phys.*, **150,** 139 (1991).
11. N. Russo and D. R. Salahub, Eds., *Metal Ligand Interaction: Structure and Reactivity*, Kluwer, Dordrecht, 1995.
12. J. M. Seminario and P. Politzer, Eds., *Density Functional Theory: A Tool for Chemistry*, Elsevier, New York, 1995.
13. D. P. Chong, Ed., *Recent Advances in Density Functional Methods, Vol. 1*, World Scientific, Singapore, 1995.
14. M. M. Davidson, I. H. Hillier, R. J. Hall, and N. A. Burton, *Mol. Phys.*, **83,** 327 (1994).
15. A. Fortunelli and J. Tomasi, *Chem. Phys. Lett.*, **231,** 34 (1994).
16. J. L. Chen, L. Noodleman, D. A. Case, and D. Bashford, *J. Phys. Chem.*, **98,** 11059 (1994).
17. G. J. Tawa, R. L. Martin, L. R. Pratt, and T. V. Russo, *J. Phys. Chem.*, **100,** 1515 (1996).
18. M. Cossi, V. Barone, R. Cammi, and J. Tomasi, *Chem. Phys. Lett.*, **255,** 327 (1996).
19. A. St. Amant, Ph.D. thesis, Université de Montreal, 1992.
20. W. Kohn and L. J. Sham, *Phys. Rev.*, **A140,** 1133 (1965).
21. H. Hoshi, M. Sakurai, Y. Inoue, and Chûjo, *J. Chem. Phys.*, **87,** 1107 (1987).
22. H. Hoshi, M. Sakurai, Y. Inoue, and Chûjo, *J. Mol. Struct.* (*Theochem*), **180,** 267 (1988).
23. J. L. Pascual-Ahuir, E. Silla, and I. Tunon, *J. Comput. Chem.*, **15,** 1127 (1994).
24. M. Cossi, B. Mennucci, and R. Cammi, *J. Comput. Chem.*, **17,** 57 (1996).
25. R. A. Pierotti, *Chem. Rev.*, **76,** 717 (1976).
26. J. Caillet and P. Claverie, *Acta Cryst.*, **B34,** 3266 (1978).
27. F. M. Floris and J. Tomasi, *J. Comput. Chem.*, **10,** 616 (1989); F. M. Floris, J. Tomasi, and J. L. Pascual-Ahuir, *J. Comput. Chem.*, **12,** 784 (1991).
28. S. H. Vosko, L. Wilk, and M. Nusair, *Can. J. Phys.*, **58,** 1200 (1980).
29. J. P. Perdew, *Phys. Rev.*, **B33,** 8822 (1986).
30. J. P. Perdew and Y. Wang, *Phys. Rev.*, **B33,** 8800 (1986).
31. N. Godbout, D. R. Salahub, J. Andzelm, and E. Wimmer, *Can. J. Chem.*, **70,** 560 (1992).
32. D. F. Shanno, *Math. Comp.*, **24,** 647 (1970), and references therein.
33. H. A. Carlson, T. B. Nguyen, M. Orozco, and W. Jorgensen, *J. Comput. Chem.*, **14,** 1240 (1993).
34. D. R. Lide, Ed., *Handbook of Chemistry and Physics*, CRC Press, Boca Raton, FL, 1991.
35. R. G. Pearson, *J. Am. Chem. Soc.*, **108,** 6109 (1986).
36. A. Bondi, *J. Phys. Chem.*, **68,** 441 (1964).
37. R. C. Weast, Ed., *Handbook of Chemistry and Physics, 72th Ed.*, CRC Press, Cleveland, OH, 1981.
38. S. Tucker and D. J. Truhlar, *J. Phys. Chem.*, **93,** 8138 (1989).
39. S. R. Vande Linde and W. L. Hase, *J. Am. Chem. Soc.*, **111,** 2349 (1989).
40. S. Tucker and D. J. Truhlar, *J. Am. Chem. Soc.*, **112,** 3338 (1990).
41. B. D. Wladkowski, K. F. Lim, W. D. Allen, and J. I. Brauman, *J. Am. Chem. Soc.*, **114,** 9136 (1992).
42. L. Deng, V. Branchadell, and T. Ziegler, *J. Am. Chem. Soc.*, **116,** 10645 (1994).
43. S. E. Barlow, J. M. Van Doren, and V. M. Bierbaum, *J. Am. Chem. Soc.*, **110,** 7240 (1988).
44. J. W. Larson and T. B. McMahon, *J. Am. Chem. Soc.*, **107,** 766 (1985).
45. W. J. Albery, *Annu. Rev. Phys. Chem.*, **31,** 227 (1980).
46. W. J. Albery and M. M. Kreevoy, *Adv. Phys. Org. Chem.*, **16,** 87 (1978).

47. T. N. Truong and E. V. Stafanovich, *J. Phys. Chem.*, **99,** 14700 (1995).
48. J. Gao, *J. Am. Chem. Soc.*, **113,** 7796 (1991).
49. *JANAF Thermochemical Tables*, 3*rd Ed., Vols. 11 and 14*, 1985.
50. M. Sola, A. Lledos, M. Duran, J. Bertran, and J. M. Abboud, *J. Am. Chem. Soc.*, **113,** 2873 (1991).
51. J. Gao and X. Xia, *J. Am. Chem. Soc.*, **115,** 9667 (1993).
52. M. H. Abraham, *Prog. Phys. Org. Chem.*, **11,** 1 (1974).
53. R. A. Back, *Rev. Chem. Intermed.*, **5,** 293 (1984).
54. H. R. Tang and D. M. Stambury, *Inorg. Chem.*, **33,** 1388 (1994).
55. M. L. McKee, *J. Phys. Chem.*, **97,** 13608 (1993).
56. R. A. Back, C. Willis, and D. A. Ramsay, *Can. J. Chem.*, **52,** 1006 (1974).
57. T. Mineva, N. Russo, and M. Toscano, *Int. J. Quantum Chem.*, **56,** 663 (1995).